Journal of Materials Chemistry C

RSC Publishing

PAPER

View Article Online
View Journal | View Issue



Cite this: J. Mater. Chem. C, 2013, 1, 7736

# All-polymer field-effect transistors using a brush gate dielectric†

Ana B. Rodríguez,[a] Michael R. Tomlinson,[a] Saghar Khodabakhsh,[b] Jui-Fen Chang,‡[c] Fabrice Cousin,[d] Dieter Lott,[e] Henning Sirringhaus,[c] Wilhelm T. S. Huck,§[b] Anthony M. Higgins[f] and Mark Geoghegan*[a]

Received 5th June 2013
Accepted 9th September 2013

DOI: 10.1039/c3tc31076k

www.rsc.org/MaterialsC

Interfaces between a poly(3-hexylthiophene) [P3HT] and an end-grafted (brush) layer of poly(methyl methacrylate) [PMMA] are shown using neutron reflectometry to be dependent on heat treatment. Annealing the samples allows part of the brush layer to cross into the P3HT layer creating a very asymmetric interface. We suggest that the P3HT rearrangement occurs, creating space for movement of the brush into the film. This interpenetration was observed with two different molecular weight (17.5 and 28 kg mol$^{-1}$) P3HT films. Output characteristics of devices made from P3HT layers on PMMA brushes show that different amounts of heat treatment do not significantly change the device performance. Saturated hole mobilities are dependent on heat treatment, with devices made from a smaller molecular weight P3HT (22 kg mol$^{-1}$) demonstrating larger mobilities than devices created using 48 kg mol$^{-1}$ P3HT, but only after heat treatment.

## 1 Introduction

All-polymer field-effect transistors (FETs) have been developed for a number of years due to their impressive processability and to further improve development of flexible devices. The lack of a need for expensive fabrication facilities is a major advantage, but ease of preparation of devices is also of some importance.[1,2] A facile means of creating all-polymer devices is to spin-coat the active layer onto the gate dielectric, but each polymer layer requires a different solvent, with a solubility orthogonal to that of the preceding layer to prevent dissolution of the device during preparation.[3,4] Such a limitation has restricted the use of solvent cast films for all-polymer devices.

Optimal transistor performance requires layers with complete integrity as well as interfaces free of traps. This is particularly true in the case of the dielectric layer, because leakage and short-circuiting are caused by imperfections and pinhole defects. Although making thicker dielectric layers is more likely to provide layer integrity, longer channel lengths, $L$ are required, since $L_{\min} \propto t_\varepsilon$, where $t_\varepsilon$ is the thickness of the gate dielectric and $L_{\min}$ is the minimum channel length appropriate for that dielectric thickness. The shorter the channel, the more difficult it becomes to control ("pinch off") the flow of carriers in the semiconductor, and a thinner gate layer is required. It is important to have the gate layer as thin as possible in order that a smaller gate voltage be required to maintain the required charge density at the interface.[5,6]

The use of surface-grafted polymers conveys inherent advantages in the creation of polymer transistors.[7,8] To graft a polymer from the surface first requires an initiator layer, which self-assembles on the surface. A gold electrode presents an ideal surface for thiol-terminated initiators. The surface must be imperfection free to support complete coverage by the initiator. During synthesis, the polymer is grown *in situ* from the surface allowing a high grafting density to be achieved. The resultant close packing of the chain ends results in a stretched polymer conformation, which gives rise to the descriptive term "polymer brush". Because the brush has been chemically grafted onto the substrate, the deposition of the next layer by solvent casting will not remove the grafted polymer. This does not mean that orthogonal solvents are no longer preferable, but it does mitigate the problem of layer dissolution and possibly also of poor

[a]Department of Physics and Astronomy, University of Sheffield, Sheffield S3 7RH, UK. E-mail: mark.geoghegan@sheffield.ac.uk
[b]Melville Laboratory for Polymer Synthesis, Department of Chemistry, University of Cambridge, Lensfield Road, Cambridge, CB2 1EW, UK
[c]Department of Physics, Cavendish Laboratory, J. J. Thomson Avenue, Cambridge CB3 0HE, UK
[d]Laboratoire Léon Brillouin, CEA-CNRS UMR12, CE-Saclay, F-91191 Gif-sur-Yvette Cédex, France
[e]Institute for Materials Research, GKSS-Forschungszentrum Geesthacht, D-21502 Geesthacht, Germany
[f]College of Engineering, Swansea University, Swansea SA2 8PP, UK

† Electronic supplementary information (ESI) available: Contains the output characteristics for all devices measured and tabulated device data. See DOI: 10.1039/c3tc31076k

‡ Present address: Department of Optics and Photonics, National Central University, Jhongli, Taoyuan 32001, Taiwan.
§ Present address: Institute for Molecules and Materials, Radboud University Nijmegen, Nijmegen 6525, Netherlands.

device performance due to mixing or roughness at the interface between the dielectric and active layers.[4,9] The dielectric layer is therefore more chemically robust when grafted from a surface. It can be expected for a polymer brush dielectric that intimate mixing at the interface with the active layer would be suppressed due to the entropic penalty incurred by the further stretching of the brush molecules and significant interpenetration into the active layer. The use of brush gate layers has been demonstrated previously for different systems.[7,8] In our earlier work,[7] we demonstrated the use of atom transfer radical polymerization (ATRP) as a means to grow poly(methyl methacrylate) (PMMA) gate dielectric layers from a gold surface. Here we develop the theme and discuss the performance of devices made of a poly(3-hexylthiophene) (P3HT) active layer on PMMA brush layers for two different P3HT molecular masses.

## 2 Materials and methods

### 2.1 Brush synthesis

The PMMA brush layers were prepared by a "grafting-from" ATRP synthesis. Silicon wafers of 5 mm thickness and 5 cm diameter were employed for the neutron reflectometry experiments. For the fabrication of the electronic devices, a sample geometry of $SiO_2$/PMMA/P3HT/gold was used. The gate dielectric brush was grown using ATRP on 0.5 $cm^2$ thin silicon wafers for the electronic devices. The substrates were cleaned by three solvent sonication (water, acetone, and methanol) followed by oxygen plasma cleaning. The substrates were then immersed overnight in a dilute anhydrous toluene solution of (11-(2-bromo-2-methyl)propionyloxy) undecyltrichlorosilane (the initiator for surface ATRP) held at −10 °C, which allowed a self-assembled monolayer of the initiator to be formed.

The PMMA brushes were grown for up to 30 h in a solution containing 2.7 mL MMA, 0.051 g CuCl, 1 mg $CuCl_2$, and 0.173 g 2,2′-bipyridine dissolved in a mixture of 2.7 mL methanol and 0.55 mL deionized water. The time allowed for the brushes to grow affected their final thickness (a maximum of 70 nm) but not the grafting density. During the growth process, the sample was kept at room temperature for different times, depending on the desired thickness for the brush. Polymer brushes were cleaned by light rinsing with acetone and propan-2-ol, after a brief sonication in water.

For the neutron reflectivity samples, deuterated monomer was used in the brush synthesis. The resulting (dPMMA) brushes have a significantly larger scattering length density than the semiconducting P3HT layers above them, enabling the interfacial structure to be assessed. P3HT was deposited by spin coating from chloroform (which is also a good solvent for PMMA), with two different molecular weights used: 17.5 kg $mol^{-1}$ (P3HT17; with regio-regularity >90% as stated by the supplier, Sigma Aldrich) and 28 kg $mol^{-1}$ (P3HT28; with stated regio-regularity of between 95 and 98% from American Dye Source).

### 2.2 Neutron reflectometry

Neutron reflectometry measurements were made using the time-of-flight EROS reflectometer of the Orphée reactor at the Laboratoire Léon Brillouin, or the monochromatic NERO reflectometer at the Geesthacht reactor. Neutrons are scattered by atomic nuclei with the neutron scattering length determining the magnitude of the interaction. Neutron reflectometry enables a determination of the scattering length density as a function of depth. Contrast between different organic components is generally obtained by deuterium labelling one component (in our case, the PMMA gate dielectric), although other components, such as gold have large enough scattering length densities to provide contrast with non-deuterated organic layers.

For the NERO reflectometer, a graphite focussing monochromator crystal was used to diffract cold neutrons with a wavelength of 0.433 nm, which were collimated through different slits. The sample can be moved in the horizontal direction and rotated in order to achieve a maximum momentum transfer vector $Q = 2.2$ $Å^{-1}$. A $^3$He pencil counter was employed for neutron detection.

The EROS reflectometer consisted of a 3.9 mm collimator, which defined the narrow neutron beam (0.3 nm < $\lambda$ < 2.5 nm, where $\lambda$ is the neutron wavelength), and supermirrors, which direct the beam towards the sample. All measurements were taken using two angles to cover the desired range of $Q$. Again, a simple $^3$He detector was used for neutron detection.

Data were fitted using a multilayer model and fitting parameters optimized using a downhill simplex routine.[10] The scattering length densities of the components were allowed to float from their expected values. The scattering length densities of the silicon substrate and P3HT film were restricted within a small range ($\pm 0.5 \times 10^{-6}$ $Å^{-2}$) of their expected values. In fact, the fitting was insensitive to the P3HT, for which the expected scattering length density is $\sim 0.5 \times 10^{-6}$ $Å^{-2}$. The scattering length density of the dPMMA brushes were allowed to float in the fitting procedure to allow for variation in the level of deuteration of the monomer. It is also possible that the brush density was less than that of molten PMMA (1.17 g $cm^{-3}$) due to stoichiometric constraints. Neither of these uncertainties were of critical importance, because we found the scattering length density of the dPMMA to lie consistently between 5.2 and 5.3 × $10^{-6}$ $Å^{-2}$, which corresponds to six deuterons per monomer.

### 2.3 Device preparation and measurement

For the FET measurements, P3HT was deposited by spin coating from chloroform solution (10 mg $mL^{-1}$) to create a ~100 nm layer. Two different P3HT samples were used with molecular weights of 22 kg $mol^{-1}$ (P3HT22; with a stated dispersity of 1.6) and 42 kg $mol^{-1}$ (P3HT42; with a stated dispersity of 1.8). Both samples were obtained from Merck with regio-regularity of better than 97%. Gold source and drain electrodes were then evaporated using a shadow mask. The channel length of the devices was kept within 60 μm < $L$ < 120 μm and the device width was $W = 1.5$ mm.

The electrical properties of the PMMA brush layers were also characterized using capacitance experiments. After cleaning PMMA brushes (grown on a 300 nm-thick silicon dioxide layer), a layer of P3HT was deposited to create a metal–insulator–semiconductor (MIS) geometry. Capacitance–voltage ($C$–$V$)

measurements were performed by varying the d.c. bias applied to the gate electrode from −35 V to 35 V, with the a.c. bias amplitude fixed at 1 V and the modulation frequency at 37 Hz.

## 3 Results and discussion

### 3.1 Neutron reflectometry measurements

Samples were made with brush thicknesses of between 40 and 67 nm. The equilibrium structure of the interface between two polymer layers is, in general, dependent on the thickness of the two layers.[11] However, here, we make no claim that the interfaces that we measured between the two components after annealing at the stated temperature were at equilibrium. The grafting density was kept constant, and would be expected to be of the order of 0.5 brushes per nm$^2$ in comparison with similar systems.[12,13] (Direct measurement of grafting density is unreliable, but an accurate knowledge of grafting density is unimportant in the present study.) We present data for different annealing treatments for these brushes, at temperatures above and below the glass transition of PMMA.

Neutron reflectometry data are shown in Fig. 1 for unannealed samples for the different brushes and P3HT samples. The quality of the fits is good with $10 < \chi^2 < 20$. In all cases the roughness of the dPMMA/P3HT interface is between 3.3 and 4.4 nm, with no systematic dependence on brush thickness. This is a narrow range for unannealed samples of this nature. It demonstrates that the synthetic procedure used is reproducible, and that the brushes are of good quality, with a thickness-independent roughness. The unannealed samples have relatively sharp interfaces between the brush and P3HT, which indicates that the casting of the P3HT from chloroform does not result in significant swelling of the brush, which would have caused significant interfacial broadening.

Having established the reproducibility of the brush layer, samples were annealed for different periods. In Fig. 2, we show volume fraction-depth profiles for some samples at different temperatures and annealing times. It is clear that annealing has an important effect on film morphology, although there is no clear effect of the molecular mass of the P3HT. The deformation of the interface was not observed on any of the as-cast samples, and is therefore a consequence of the annealing process. Changes in interfacial structure in these bilayers are due to either lateral roughness (for example, caused by capillary waves at a liquid–liquid interface), or interpenetration of at least one component into the other. We propose that interpenetration of the P3HT layer by the brush is most likely to be the cause of what is observed here; the P3HT cannot easily penetrate the dPMMA brush because the brush would have difficulty swelling to accommodate it. Capillary waves have a sinusoidal or near-sinusoidal interfacial profile, and so are not responsible for the structure observed here. Furthermore, the length scale of the interpenetration is too large for capillary waves (unless the sample dewetted), and in any case, the P3HT is expected to have large regions of crystallinity[14,15] which could not be treated as a liquid surface, and thus exhibit such capillary waves. The step-like shape of the profile allows speculation that the dPMMA is penetrating grain boundaries and other defects in crystalline regions of the P3HT. Certainly, P3HT exhibits crystalline behaviour at the annealing temperatures performed here, even down to 40 °C.[16] The exact molecular mechanisms of

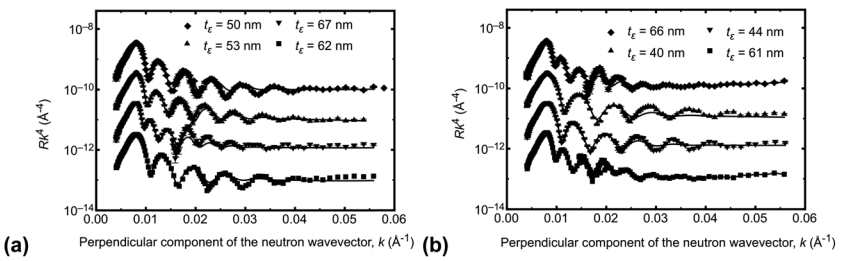


**Fig. 1** Reflectivity g per molta and fits for (unannealed) samples of (a) P3HT17 and (b) P3HT28 on dPMMA brushes of different thickness, $t_\varepsilon$. The data are plotted as $Rk^4(k)$ to allow a better assessment of the quality of the fits, and the data are staggered by factors of 10 for purposes of clarity.

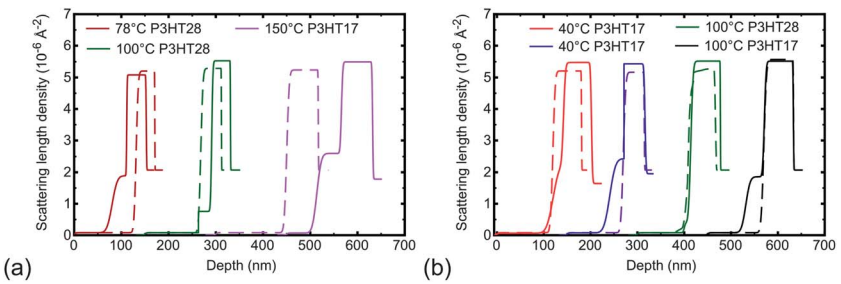


**Fig. 2** Scattering length density as a function of depth for P3HT on dPMMA brushes after annealing for (a) 5 min and (b) 24 h. Data are offset horizontally for clarity, and dashed lines are for the corresponding unannealed samples. The silicon substrate is to the right of each profile, and the P3HT layer on the left hand side. Two different samples are shown for P3HT17 annealed for 24 h at 40 °C. These allow for a test of reproducibility.

 

how such structural rearrangements can proceed is difficult to understand given that PMMA has a glass transition temperature in excess of 100 °C. It is known that thin films of PMMA on gold exhibit depressed glass transition temperatures,[17] but the effects of the (molecular) mobility of amorphous polymers below the glass transition contains many open questions.

In Fig. 3 Scanning force microscopy (SFM) images (obtained in tapping mode using a MultiMode Digital Instruments atomic force microscope) of three samples are shown. An as-cast film on a silicon substrate (Fig. 3a) is notably rough, but the annealed films are smoother. The large roughness seen in the as-cast surface in Fig. 3a is a (non-equilibrium) remnant of the spin-coating process. The amplitude of this roughness greatly reduces on annealing as seen in Fig. 3b and c. For these annealed samples (Fig. 3b and c), which have different P3HT films on the PMMA brushes, similar results are observed. Isolated defects are apparent in the annealed structures in Fig. 3b and c, taking the form of depressions in the surface of the order of a few nanometres. The origin of these defects is not clear; their small size means that they may even be present in the unannealed samples. Because these defects have a depth that is much less than the typical brush thickness, they do allow some brush penetration, but this should not affect the integrity of the device. Aside from these defects, the surface is otherwise considerably smoother than the as-cast film. We do not have information on the (buried) P3HT interface with the polymer brush, but experimental studies of different P3HT interfaces have previously been reported and there can be more or less crystallinity at the buried interface compared to the free surface, depending on the surface in which the P3HT contacts.[18] Regioregularity and molecular weight play key roles in the degree of crystallinity, and the orientation of crystalline lamellae in P3HT thin films.[19] Previous work, in which P3HT is spin-coated from a variety of solvents onto different substrates,

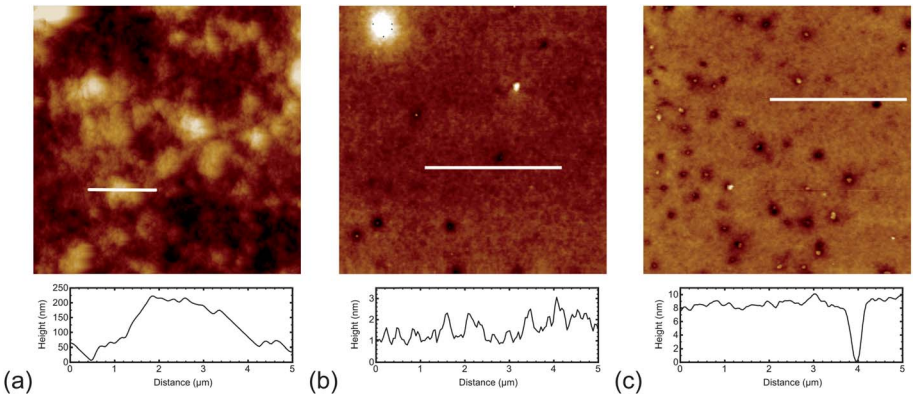


**Fig. 3** Scanning force microscopy images of P3HT layers: (a) P3HT17 unannealed spin-coated onto a silicon substrate; (b) P3HT17 annealed at 100 °C for 24 h; and (c) P3HT28 annealed at 100 °C for 24 h. 5 μm height scans are indicated for the region covered by the white line in each image.

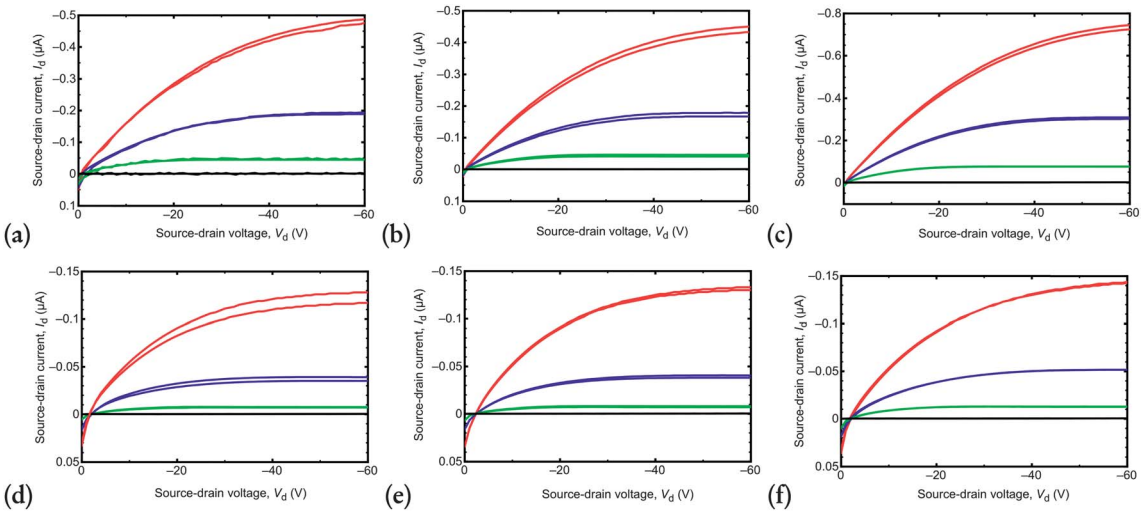


**Fig. 4** Output characteristics of P3HT22 (a–c) and P3HT42 (d–f) FETs with PMMA brushes on $SiO_2$ as gate insulators. (a) and (d) Reference samples, using a 700 nm-thick PMMA film spin-coated from *n*-butyl acetate rather than a brush, and with no heat treatment before or after P3HT deposition (threshold voltage, $V_T = -5.6$ and $-13.3$ V respectively); (b) and (e) samples annealed at 40 °C for 24 h ($V_T = -7.2$ and $-14.6$ V respectively); and (c) and (f) samples annealed at 100 °C for 5 min ($V_T = -0.3$ and $-9.8$ V respectively). The gate voltages are $V_g = 0$, $-20$, $-40$, and $-60$ V and are indicated by red, blue, green, and black curves respectively. Threshold voltages are obtained from the $I_d^{1/2}(V_g)$ transfer characteristics in the saturated regime ($V_d = -60$ V).

has shown (for the ranges of molecular weights and regioregularity that we have used in the present study) that the P3HT (100) direction is usually normal to the substrate in blends, bilayers and pure P3HT layers.[15,18–22] Annealing does not affect this crystal orientation with respect to the substrate, but has the effect of increasing the volume fraction of crystalline regions and the crystallite size and perfection.[20] In the present study we do not know how the mixing at the interface affects the crystalline structure, but previous studies have shown that mixing within the amorphous P3HT fraction in a bilayer geometry, does not disrupt the organisation of the crystalline P3HT domains.[22]

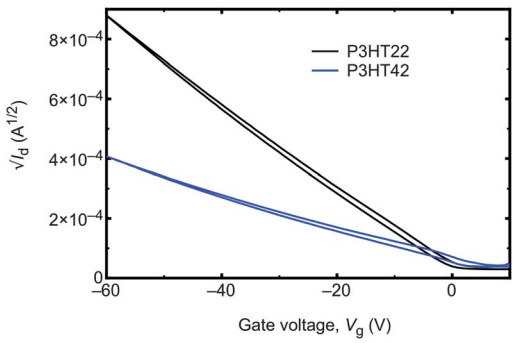


**Fig. 5** Transfer characteristics for samples with P3HT brushes on $SiO_2$ as gate insulators after annealing at 100 °C for 24 h ($V_T = -0.3$ and 4.4 V for the P3HT22 and P3HT42 respectively). In these experiments, $V_d = -60$ V.

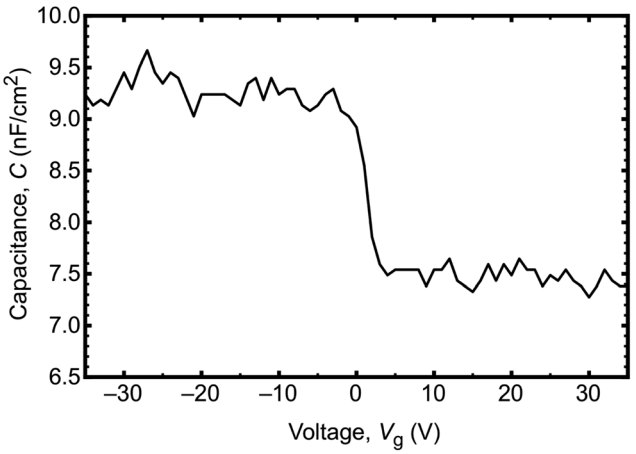


**Fig. 6** Capacitance (*C*–*V*) results for a PMMA brush grown from a (300 nm) silicon dioxide layer. These data were obtained using P3HT42 as the semiconductor layer.

### 3.2 Output characteristics

In order to determine whether the structural evolution of the interface upon annealing has any practical consequences for real devices, the output characteristics for devices fabricated with two different P3HT molecular weights are shown in Fig. 4. The thin dielectric allows these devices to operate at low voltages (less than 5 V). Transfer characteristics reveal threshold voltages, $V_T$, that are typically between 0 and 10 V, and these are noted for some devices in the caption to Fig. 4. (All are included in the ESI.†) Example transfer characteristics are shown in Fig. 5. Generally, the devices using P3HT22 provide the smallest values of $V_T$. Furthermore, these devices also have significantly better output characteristics, suggesting that the effective capacitance of the brush layer is reduced due to traps in the P3HT42-based devices, possibly due to a less effective active layer. Certainly the quality of the P3HT film is playing an important role in the device behaviour.

The *C*–*V* measurements (Fig. 6) indicate a low turn-on voltage. The sharp slope at $V_g = 0$ indicates a low trap density. The areal capacitance measured at $V_g = -35$ V is normalized to the calculated value of 9.2 ± 0.2 nF cm$^{-2}$, which is for PMMA grown on silicon dioxide. The mobilities obtained from the transfer characteristics, for both long and short time annealing and for the two different molecular weights of P3HT tested, as well as reference unannealed devices are shown in Fig. 7. Values for carrier mobilities are found in the range of $3 \times 10^{-4}$ to $2 \times 10^{-3}$ V cm$^{-1}$ s$^{-1}$, with the annealing treatment affecting the P3HT42 samples more than the P3HT22 samples. In earlier studies using a silicon dioxide gate dielectric,[23,24] it was noted that smaller mobilities are found for the lower molecular weight P3HT, in contrast to what we observe here. We do note, however, that the mobilities are of a similar order of magnitude to those in the earlier work, and also that the polymers in the earlier work were of lower molecular weights than those we have used here.[23] More recent research has shown that P3HT mobility in space-charge-limited current devices is greatest at a P3HT (number average) molecular weight of 12 kg mol$^{-1}$.[25]

The performance of the devices after annealing at 40 °C is similar, indicating that the P3HT is of a similar quality. However, the mobility of the P3HT42 decreases with annealing

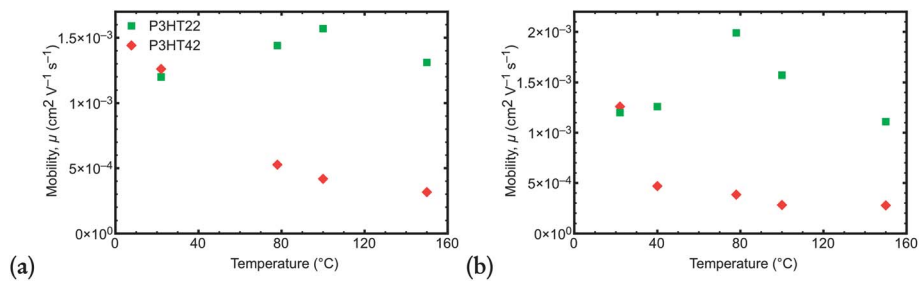


**Fig. 7** Saturated hole mobility data as a function of annealing temperature for 5 minutes annealing (a) and for 24 h annealing (b). The samples "annealed" at 22 °C are unannealed reference samples (a 700 nm spin coated PMMA layer rather than a brush); the temperature represents room temperature.

 

whilst that of the P3HT22 sample is a little larger than the reference sample on the 700 nm PMMA film, although no systematic temperature dependence can be stated. The likelihood here is that the shorter P3HT is better able to order due its larger (molecular) mobility during annealing.

It should not be concluded that a rough interface, or one with a complex structure, would result in a device of poor quality. Recent work has shown that non-uniform interfaces do not preclude good performance when P3HT is blended with an amorphous polymer.[26] Our system may well have an interfacial structure not very different to the blend study, which indicates that the main requirement being that any crystalline regions of P3HT be connected to each other well enough through, for example, tie-lines or amorphous regions of P3HT.[26]

## 4 Conclusions

We have used neutron reflectometry to demonstrate that a PMMA brush gate dielectric will penetrate the active P3HT layer after annealing, even at temperatures as low as 40 °C. Device performance has been measured and output characteristics are not adversely affected by heat treatment. It is known that the addition of amorphous polymers into the active layers of organic FETs does not necessarily adversely affect device performance[27] and this is supported by the neutron data illustrating the penetration of the active layer by the gate. Saturated hole mobilities are, however, affected by heat treatment, with one sample exhibiting a small increase in mobility compared to the reference sample, and the other with a decrease in mobility on increased annealing.

## Acknowledgements

We acknowledge the EPSRC for funding through GR/S96920/01. This project was supported by the European Commission under the 6th Framework Programme through the Key Action: Strengthening the European Research Area, Research Infrastructures (RII3-CT-2003-505925).

## References

1 Z. Bao, *Adv. Mater.*, 2000, **12**, 227–230.
2 H. Klauk, *Chem. Soc. Rev.*, 2010, **39**, 2643–2666.
3 K.-J. Baeg, A. Facchetti and Y.-Y. Noh, *J. Mater. Chem.*, 2012, **22**, 21138–21143.
4 S. S. Chang, A. B. Rodríguez, A. M. Higgins, C. Liu, M. Geoghegan, H. Sirringhaus, F. Cousin, R. M. Dalgliesh and Y. Deng, *Soft Matter*, 2008, **4**, 2220–2224.
5 Y.-Y. Noh, N. Zhao, M. Caironi and H. Sirringhaus, *Nat. Nanotechnol.*, 2007, **2**, 784–789.
6 J. Veres, S. Ogier and G. Lloyd, *Chem. Mater.*, 2004, **16**, 4543–4555.
7 J. C. Pinto, G. L. Whiting, S. Khodabakhsh, L. Torre, A. B. Rodríguez, R. M. Dalgliesh, A. M. Higgins, J. W. Andreasen, M. M. Nielsen, M. Geoghegan, W. T. S. Huck and H. Sirringhaus, *Adv. Funct. Mater.*, 2008, **18**, 36–43.
8 I. M. Rutenberg, O. A. Scherman, R. H. Grubbs, W. Jiang, E. Garfunkel and Z. Bao, *J. Am. Chem. Soc.*, 2004, **126**, 4062–4063.
9 L.-L. Chua, P. K. H. Ho, H. Sirringhaus and R. H. Friend, *Adv. Mater.*, 2004, **16**, 1609–1615.
10 R. A. L. Jones, L. J. Norton, K. R. Shull, E. J. Kramer, G. P. Felcher, A. Karim and L. J. Fetters, *Macromolecules*, 1992, **25**, 2359–2368.
11 M. Sferrazza, C. Xiao, R. A. L. Jones, D. G. Bucknall, J. Webster and J. Penfold, *Phys. Rev. Lett.*, 1997, **78**, 3693–3696.
12 S. Edmondson, V. L. Osborne and W. T. S. Huck, *Chem. Soc. Rev.*, 2004, **33**, 14–22.
13 B. Zhao and W. J. Brittain, *Prog. Polym. Sci.*, 2000, **25**, 677–710.
14 M. Brinkmann, *J. Polym. Sci., Part B: Polym. Phys.*, 2011, **49**, 1218–1233.
15 E. Verploegen, R. Mondal, C. J. Bettinger, S. Sok, M. F. Toney and Z. Bao, *Adv. Funct. Mater.*, 2010, **20**, 3519–3529.
16 Y. Zhao, G. Yuan, P. Roche and M. Leclerc, *Polymer*, 1995, **36**, 2211–2214.
17 J. L. Keddie, R. A. L. Jones and R. A. Cory, *Faraday Discuss.*, 1994, **98**, 219–230.
18 W. Porzio, C. Scavia, L. Barba, G. Arrighetti and S. Milita, *Eur. Polym. J.*, 2011, **47**, 273–283.
19 H. Sirringhaus, P. J. Brown, R. H. Friend, M. M. Nielson, K. Bechgaard, B. M. W. Langeweld-Voss, A. J. H. Spiering, R. A. J. Janssen, E. W. Meijer, P. Herwig and D. M. de Leeuw, *Nature*, 1999, **401**, 685–688.
20 H. W. Ro, B. Akgun, B. T. O'Connor, M. Hammond, R. J. Kline, C. R. Snyder, S. K. Satija, A. L. Ayzner, M. F. Toney, C. L. Soles and D. M. DeLongchamp, *Macromolecules*, 2012, **45**, 6587–6599.
21 S. T. Salammal, E. Mikayelyan, S. Grigorian, U. Pietsch, N. Koenen, U. Scherf, N. Kayunkid and M. Brinkmann, *Macromolecules*, 2012, **45**, 5575–5585.
22 N. D. Treat, M. A. Brady, G. Smith, M. F. Toney, E. J. Kramer, C. J. Hawker and M. L. Chabinyc, *Adv. Energy Mater.*, 2011, **1**, 82–89.
23 R. J. Kline, M. D. McGehee, E. N. Kadnikova, J. Liu and J. M. J. Fréchet, *Adv. Mater.*, 2003, **15**, 1519–1522.
24 A. Zen, J. Pflaum, S. Hirschmann, W. Zhuang, F. Jaiser, U. Asawapirom, J. P. Rabe, U. Scherf and D. Neher, *Adv. Funct. Mater.*, 2004, **14**, 757–764.
25 C. R. Singh, G. Gupta, R. Lohwasser, S. Engmann, J. Balko, M. Thelakkat, T. Thurn-Albrecht and H. Hoppe, *J. Polym. Sci., Part B: Polym. Phys.*, 2013, **51**, 943–951.
26 G. Lu, J. Blakesley, S. Himmelberger, P. Pingel, J. Frisch, I. Lieberwirth, I. Salzmann, M. Oehzelt, R. di Pietro, A. Salleo, N. Koch and D. Neher, *Nat. Commun.*, 2013, **4**, 1588.
27 M.-B. Madec, D. Crouch, G. Rincon Llorente, T. J. Whittle, M. Geoghegan and S. G. Yeates, *J. Mater. Chem.*, 2008, **18**, 3230–3236.